BER Performance of OFDM-MDPSK System in Frequency-Selective Rician Fading with Diversity Reception

Jun Lu, Tjeng Thiang Tjhung, *Senior Member, IEEE,* Fumiyuki Adachi, *Senior Member, IEEE,* and Cheng Li Huang

***Abstract*—A closed form formula is derived for the bit error rate (BER) of orthogonal-frequency-division-multiplexing (OFDM) with M-ary differential-phase-shift-keying (MDPSK) systems in frequency-selective Rayleigh and Rician fading channels with diversity reception. New BER curves are obtained as a function of the rms delay spread of the diffused component for three different types of delay profiles: 1) one-sided exponential, 2) uniform and 3) double spike profiles. Both slow and fast fading conditions are considered. It is shown that the existence of a strong line-of-sight (LOS) component and the use of reception diversity can effectively improve transmission performance.**

***Index Terms*—Bit error rate, delay spread, Doppler shift, frequency-selective Rician fading, MDPSK modulation, OFDM system.**

I. Introduction

MOBILE radio communication systems are increasingly required to provide a variety of high-quality multimedia services to mobile users. To meet these demands, modern mobile radio transceiver systems must be able to support high capacity and variable bit rate information transmission and with high bandwidth efficiency to conserve the limited spectrum resource. However, in the mobile radio environment, signals are usually impaired by fading and multipath delay phenomenon. In such channels, severe fading of the signal amplitude and inter-symbol-interference (ISI) due to the frequency-selectivity of the channel lead to an unacceptable degradation of the error performance.

Adaptive equalization techniques have been widely used in the single carrier mobile communication systems to combat fading and multipath delay effects. However, long time delays, i.e., several symbols, requires very complex equalization process (Viterbi equalization requires M^{n+1} state Viterbi algorithm, where M is the number of modulation levels and n is the number of ISI symbols), and because of the high cost of the hardware, there are practical difficulties to use this technique in system operating at high bit rates, e.g., up to several megabits per second.

Manuscript received February 8, 1999; revised October 13, 1999.

J. Lu and T. T. Tjhung are with the Center for Wireless Communications, National University of Singapore, TeleTech Park, Singapore Science Park II, Singapore, 117674.

F. Adachi is with NTT Mobile Communications Network Inc., Yokosuka-shi 239-8536, Japan.

C. L. Huang is with the Department of Electrical Engineering, National University of Singapore, Singapore, 119260.

Publisher Item Identifier S 0018-9545(00)04826-X.

In recent years, an innovative so-called orthogonal-frequency-division-multiplexing (OFDM) modulation scheme has been found effective for the transmission of high bit rate signals in multipath fading environment. The main feature of OFDM systems is the avoidance of multipath delay induced ISI. This is done by sending the data in parallel on a number of narrowband ISI-free subchannels. In such a system, although each subchannel operates at a low data rate to avoid the channel frequency-selectivity, the high total data rate can be achieved by using multiple carriers.

In an OFDM system, IFFT and FFT processing are used in the modulation and demodulation of the signals. One important attribute of this scheme is the spreading of a fade over many bits. Rather than having a few adjacent bits completely destroyed, we now have all the bits only slightly affected by a fade.

Moreover, the ISI can be almost completely avoided by adding a guard interval to each block of the data, provided the guard interval is longer than the maximum multipath delay of the channel. Nevertheless, the assumption that the guard interval is longer than the maximum multipath delay cannot always be satisfied. For a system with a fixed guard interval, the system may be degraded if the channel changes from the assumed condition. This case may happen in any mobile radio communications system, because the maximum delay may vary.

A scheme in which each carrier of the OFDM signal is modulated with M-ary differential-phase-shift-keying (MDPSK), so-called OFDM-MDPSK system has been standardized in the terrestrial digital audio broadcasting (DAB) system by the European Telecommunications Standards Institute (ETSI) [8]. Okada *et al.* [1] theoretically studied the bit error rate (BER) performance of OFDM-MDPSK system in Rayleigh fading and considered the time selective fading effects separately from frequency selective delay spread effects. In [2], Saito *et al.* present simulation and experimental results mainly concerning the performance of the OFDM-DQPSK system in the presence of various disturbances such as nonlinearity of the channel, multipath (ghost) signals, and interference from analog signals.

In this paper, we theoretically analyze the BER performance of the OFDM-MDPSK system in frequency-selective Rician fading channels with diversity reception. Rician fading model is suitable for suburban areas where a line-of-sight (LOS) path often exists. This may also be true for microcellular or picocellular system with cells of less than several hundred meters in radius. Rician fading is characterized by the K factor which is the power ratio of the LOS and the diffused components. It

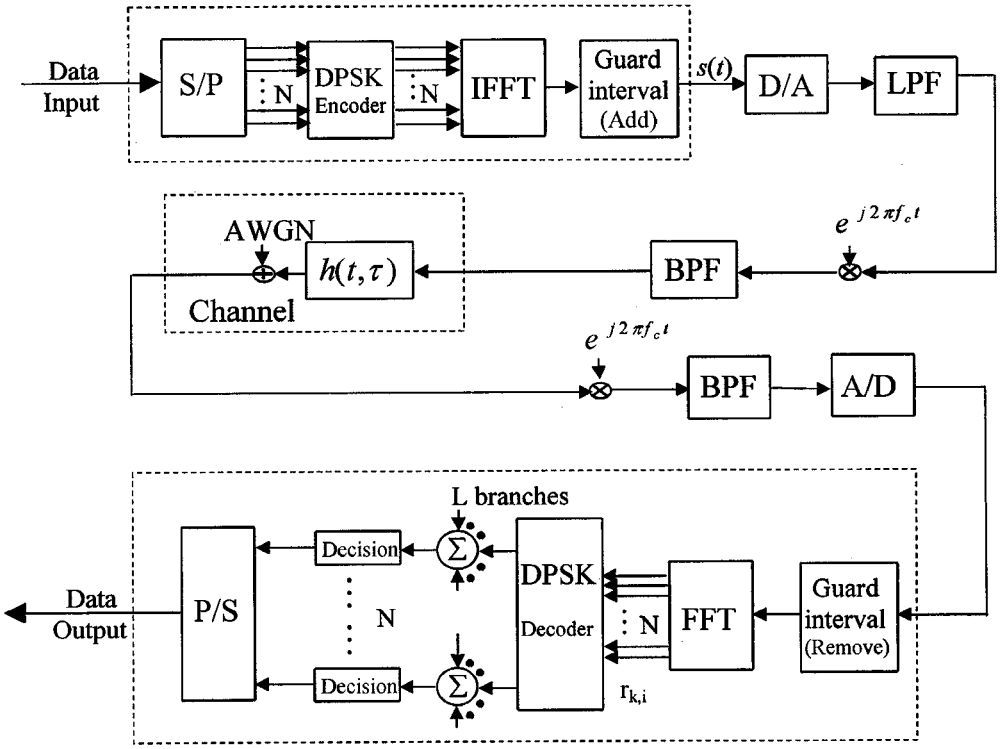

Fig. 1. Block diagram of the OFDM-MDPSK system.

represents Rayleigh fading when $K = 0$, and no fading when $K \rightarrow \infty$. Rician fading, thus, can be considered a general fading model for land mobile channels. We evaluate the error performance of each subcarrier of the OFDM system by using Proakis' analysis for the error probability for multichannel binary signals (see [3 Appendix B]). We then obtain the overall system performance by averaging the error rate of each subcarrier over the entire subchannel assembly. In the BER performance evaluation, both slow and fast fading conditions are considered with maximum ratio combining (MRC) diversity reception. Although only three different types of power delay profiles of the diffused component [one-sided exponential, uniform and double spike] are analyzed, the method presented here applies to any shape of power delay profiles.

The OFDM-MDPSK transceiver system and the fading channel model are described in Section II. The BER performance is analyzed in Section III for slow and fast fading conditions. In Section IV, BER expressions for three different power delay profiles are derived. Section V presents the error probability curves and discusses the effects of delay spread, Doppler shift, Rician factor, order of the diversity reception on the bit error probability.

II. OFDM-MDPSK Transceiver System and Fading Channel Model

The block diagram of the OFDM-MDPSK system is shown in Fig. 1. This system is similar to the transceiver model presented in [1], [2]. The serial binary information sequence is first grouped into $\log_2 M$-bit symbols, and assigned as $a_{n,i} = e^{j\Delta\phi_{n,i}}$ for the ith symbol in the nth subchannel, where $\Delta\phi_{n,i}$ is one of the M possible differential phases chosen from the constellation set $\{e^{j2\pi m/M} | m = 0, 1, \cdots, M-1\}$ using Gray bit mapping. These $a_{n,i}$'s are then parallelized by the serial-to-parallel (S/P) converter into the N subchannels. In each subchannel, the MDPSK encoder encodes each $a_{n,i}$ as $c_{n,i} = c_{n,(i-1)} \cdot a_{n,i}$ where one initial $c_{n,i}$ can be chosen arbitrarily, e.g., $c_{n,0} = e^{j0}$. For a certain i, the outputs of the MDPSK encoder are N such $c_{n,i}$'s which represent a multitone block. Then the inverse discrete Fourier transform (IDFT) is performed on the N multitone block symbols. A guard interval, which is used to reduce the interference effect caused by multipath delays, is added to each multitone block. After passing through a digital-to-analog (D/A) converter and a low pass filter (LPF), the signal is multiplied by a local radio frequency (RF) carrier and filtered by a band-pass filter (BPF) to generate the transmitted signal, which can be expressed in complex form as

$$s(t) = \sum_{i=-\infty}^{\infty} f(t - iT_b) \sum_{n=0}^{N-1} c_{n,i} e^{j2\pi f_n (t - iT_b)}. \quad (1)$$

Here, $f_n = f_c + n/t_b$ is the frequency of the nth carrier and f_c is the lowest carrier frequency. $T_b = \Delta + t_b$ is the block duration with Δ and t_b being the guard interval duration and the observation period, respectively. $f(t)$ is a symbol pulse waveform defined as [1]

$$f(t) = \begin{cases} 1 & \text{for } -\Delta \le t \le t_b \\ 0 & \text{elsewhere.} \end{cases} \quad (2)$$

Here, the D/A conversion, the low-pass filtering, up-conversion to RF signals and subsequent band-pass filtering are assumed to be ideal.

The transmitted RF signal $s(t)$ is subjected to frequency-selective Rician fading and additive white Gaussian noise (AWGN). The signal at the lth receiver branch output can be written as [1]

$$r_l(t) = \int_0^\infty s(t-\tau)h_l(t,\tau)\,d\tau + n_l(t) \tag{3}$$

where $n_l(t)$ is a complex Gaussian noise process and $h_l(t,\tau)$ is the lth channel response at time t to an impulse applied at $t-\tau$. For the frequency-selective Rician fading channels considered here, $h_l(t,\tau)$ is modeled as a LOS plus V independent Rayleigh fading paths as

$$h_l(t,\tau) = \sqrt{2P_s}\delta(\tau) + \sum_{v=1}^{V}\sqrt{P_v}h_{l,v}(t)\delta(\tau-\tau_v) \tag{4}$$

where

$\delta(\tau)$	Dirac delta function;
$h_{l,v}(t)$	independent zero-mean complex-valued Gaussian random processes with unity power [i.e., $0.5E[\lvert h_{l,v}(t)\rvert^2] = 1$] and power spectral density $S(f)$;
P_s	power of the LOS signal;
P_v and τ_v	power and delay of the vth diffused multipath component, respectively.

It is assumed that $\tau_1 < \tau_2 < \cdots < \tau_V < t_b$. The total power of the diffused multipaths is P_d and the Rician factor of the channel is thus given by

$$K = \frac{P_s}{P_d}$$

where

$$P_d = \sum_{v=1}^{V} P_v. \tag{5}$$

At the receiver, the received RF signal undergoes band-pass filtering, down conversion to baseband, low-pass filtering and analog-to-digital (A/D) conversion. These signal processing operations are assumed to be ideal also. The sampling times are ideally locked to the LOS component and the signal is received by an uncorrelated L-branch diversity receiver with MRC. After the fast Fourier transform (FFT) operation, the output of the kth subchannel at time $t = iT_b$ for the lth receiver branch can be obtained as

$$r_{l,k,i} = \frac{1}{t_b}\int_{iT_b}^{t_b+iT_b}\left\{\int_0^\infty s(t-\tau)h_l(t,\tau)\,d\tau + n_l(t)\right\} \times e^{-j2\pi f_k(t-iT_b)}\,dt, \qquad l = 1, 2\cdots, L. \tag{6}$$

Finally, the differential detector of each subchannel uses the variable $D_k = \sum_{l=1}^{L} z_{l,k,i} = \sum_{l=1}^{L} r_{l,k,i}\cdot r^*_{l,k,(i-1)}$ to decide which one of the M symbols was transmitted [3]. Then the parallel-to-serial (P/S) converter rearranges the decoded parallel data into the original binary bits for the ith multitone block.

III. BER Performance

In this section, the BER for the OFDM-MDPSK system in frequency-selective Rician fading channels with diversity reception is developed.

By substituting (1) and (4) into (6), the output of the FFT processor for the lth branch, ith multitone block and kth subchannel, $r_{l,k,i}$, can be written as

$$r_{l,k,i} = I_0 + I_1 + I_2 + I_3 + n_{l,k,i} \tag{7}$$

where

$$\begin{aligned}
I_0 &= \sqrt{2P_s}\cdot c_{k,i}\\
I_1 &= \frac{c_{k,i}}{t_b}\left\{\sum_{v=1}^{V_m} e^{-j2\pi f_k\tau_v}\sqrt{P_v}\int_{iT_b}^{iT_b+t_b} h_{l,v}(t)\,dt \right.\\
&\qquad \left. + \sum_{v=V_m+1}^{V} e^{-j2\pi f_k\tau_v}\sqrt{P_v}\int_{iT_b+\tau_v-\Delta}^{iT_b+t_b} h_{l,v}(t)\,dt\right\}\\
I_2 &= \sum_{\substack{n=0\\ n\neq k}}^{N-1}\frac{c_{n,i}}{t_b}\left\{\sum_{v=1}^{V_m} e^{-j2\pi f_n\tau_v}\sqrt{P_v}\int_{iT_b}^{iT_b+t_b} h_{l,v}(t)\right.\\
&\qquad \times e^{-j2\pi(f_n-f_k)(t-iT_b)}\,dt\\
&\qquad + \sum_{v=V_m+1}^{V} e^{-j2\pi f_n\tau_v}\sqrt{P_v}\int_{iT_b+\tau_v-\Delta}^{iT_b+t_b}\\
&\qquad \left.\times h_{l,v}(t)e^{-j2\pi(f_n-f_k)(t-iT_b)}\,dt\right\}\\
I_3 &= \sum_{n=0}^{N-1}\frac{c_{n,(i-1)}}{t_b}\\
&\qquad \times\left\{\sum_{v=V_m+1}^{V} e^{-j2\pi f_n(T_b-\tau_v)}\sqrt{P_v}\int_{iT_b}^{iT_b+\tau_v-\Delta}\right.\\
&\qquad \left.\times h_{l,v}(t)e^{-j2\pi(f_n-f_k)(t-iT_b)}\,dt\right\}
\end{aligned} \tag{8}$$

where V_m is the number of paths whose delay are less than Δ. In (7), the first term I_0 represents the desired LOS signal. The second term I_1 represents the multipath components. The third term I_2 represents the interference from other subchannels in one multitone block, which can be called inter-channel interference (ICI). The fourth term I_3 represents the interference from the previous multitone block, which can be called intersymbol interference (ISI). $n_{l,k,i}$ are statistically independent Gaussian random noise components with zero mean and one-sided power spectral density N_0.

It is to be noted that in (8), $h_{l,v}(t)$ is a zero mean complex Gaussian process, so that I_1, I_2 and I_3, which are the results of linear operations on $h_{l,v}(t)$, are Gaussian random variables. Therefore, $r_{l,k,i}$ in (7) is also a Gaussian random variable with mean I_0. We can use the results given in [3] to obtain the symbol error probability of the kth subchannel as

$$\begin{aligned}
P_s(k) = \varepsilon_M\left\{Prob\left[D_k\left(\psi = \frac{\pi}{2} - \frac{\pi}{M}\right) < 0\right]\right.\\
\left. + Prob\left[D_k\left(\psi = -\frac{\pi}{2} + \frac{\pi}{M}\right) < 0\right]\right\}
\end{aligned} \tag{9}$$

where

$$\varepsilon_M = \begin{cases} 0.5 & \text{for } M = 2 \\ 1 & \text{for } M \geq 4, \end{cases} \tag{10}$$

and

$$D_k(\psi) = \mathrm{Re}\left[\left(\sum_{l=1}^{L} r_{l,k,i} \cdot r^*_{l,k,(i-1)}\right) e^{j\psi}\right] \tag{11}$$

is a special case of a general quadratic form in complex-valued Gaussian random variables defined as in [3] as

$$D_k(\psi) = \sum_{l=1}^{L} \left[A\,|X_l|^2 + B\,|Y_l|^2 + CX_l^* Y_l + C^* X_l Y_l^*\right] \tag{12}$$

with $A = 0$, $B = 0$, $C = e^{j\psi}$, $X_l = r_{l,k,i}$ and $Y_l = r_{l,k,(i-1)}$.

Using the results in [3], we have

$$\begin{aligned} &Prob[D_k(\psi) < 0] \\ &\quad = Q(a, b) - I_0(ab)e^{-(a^2+b^2)/2} \\ &\qquad + \frac{I_0(ab)e^{-(a^2+b^2)/2}}{(1+v_1/v_2)^{2L-1}} \sum_{l=0}^{L-1} \binom{2L-1}{l} \left(\frac{v_2}{v_1}\right)^l \\ &\qquad + \frac{e^{-(a^2+b^2)/2}}{(1+v_1/v_2)^{2L-1}} \times \sum_{l=1}^{L-1} I_l(ab) \\ &\qquad \times \left\{ \sum_{k=0}^{L-1-l} \binom{2L-1}{k} \left[\left(\frac{b}{a}\right)^l \left(\frac{v_2}{v_1}\right)^k \right.\right. \\ &\qquad\qquad \left.\left. - \left(\frac{a}{b}\right)^l \left(\frac{v_2}{v_1}\right)^{2L-1-k}\right]\right\}, \qquad \text{for } L > 1 \\ &Prob[D_k(\psi) < 0] \\ &\quad = Q(a, b) - \frac{v_2/v_1}{1+v_2/v_1} I_0(ab)e^{-(a^2+b^2)/2} \\ &\qquad \text{for } L = 1 \end{aligned} \tag{13}$$

where

$$Q(a, b) = \begin{cases} e^{-(a^2+b^2)/2} \sum_{k=0}^{\infty} (a/b)^k I_k(ab), & \text{for } b > a > 0 \\ 1 - e^{-(a^2+b^2)/2} & \\ \quad \sum_{k=0}^{\infty} (a/b)^k I_k(ab), & \text{for } a > b > 0 \end{cases} \tag{14}$$

is the Marcum's Q function and $I_k(x)$ is the kth order modified Bessel function of the first kind.

In (13)

$$\begin{aligned} a &= \sqrt{\frac{2v_1^2 v_2(\alpha_1 v_2 - \alpha_2)}{(v_1+v_2)^2}}, \quad b = \sqrt{\frac{2v_1 v_2^2(\alpha_1 v_1 + \alpha_2)}{(v_1+v_2)^2}} \\ v_{1,2} &= \sqrt{w^2 + \left[|e^{j\psi}|^2 \left(m_{xx}m_{yy} - |m_{xy}|^2\right)\right]^{-1}} \mp w \\ w &= \frac{\mathrm{Re}\left(e^{j\psi} m_{xy}^*\right)}{m_{xx}m_{yy} - |m_{xy}|^2} \\ \alpha_1 &= L\left[|m_x|^2 m_{yy} + |m_y|^2 m_{xx} - 2\mathrm{Re}\left(m_x m_y^* m_{xy}^*\right)\right] \\ \alpha_2 &= 2L\mathrm{Re}\left(m_x^* m_y e^{j\psi}\right) \end{aligned} \tag{15}$$

where m_x, m_y are the means and m_{xx}, m_{yy}, and m_{xy} are the second central moments of the two complex-valued variables X_l and Y_l. Using the expression of $r_{l,k,i}$ given in (7), we can obtain these moments as

$$\begin{aligned} m_x &= E[x] = \sqrt{2P_s}\, c_{k,(i-1)}, \quad m_y = E[y] = \sqrt{2P_s}\, c_{k,i} \\ m_{xx} &= m_{yy} = 2\sum_{v=1}^{V_m} P_v \cdot R^{(1)}_{S,v} + 2 \sum_{v=V_m+1}^{V} P_v \cdot R^{(2)}_{S,v} + 2P_n \\ m_{xy} &= 2\sum_{v=1}^{V_m} P_v \cdot R^{(1)}_{C,v} + 2 \sum_{v=V_m+1}^{V} P_v \cdot R^{(2)}_{C,v} \end{aligned} \tag{16a}$$

where P_n is the power of the filtered AWGN and can be obtained as $P_n = N_0/T_b$, $R^{(1)}_{S,v}$ and $R^{(2)}_{S,v}$ are the vth coefficients of self-correlation, and $R^{(1)}_{C,v}$ and $R^{(2)}_{C,v}$ are the vth coefficients of cross-correlation of the received signal for $\tau_v < \Delta$ and $\tau_v > \Delta$, respectively. These R's can be obtained as

$$\begin{aligned} R^{(1)}_{S,v} &= \frac{1}{t_b^2}\left\{\Gamma_1(\Re) + \sum_{\substack{n=0 \\ n\neq k}}^{N-1} \Gamma_1(\Re \cdot \Lambda)\right\} \\ R^{(2)}_{S,v} &= \frac{1}{t_b^2}\left\{\Gamma_2(\Re) + \sum_{\substack{n=0 \\ n\neq k}}^{N-1} \Gamma_2(\Re \cdot \Lambda) + \sum_{n=0}^{N-1} \Gamma_3(\Re \cdot \Lambda)\right\} \\ R^{(1)}_{C,v} &= \frac{1}{t_b^2}\left\{\Gamma_4(\Re)\right\}, \quad R^{(2)}_{C,v} = \frac{1}{t_b^2}\left\{\Gamma_5(\Re)\right\} \end{aligned} \tag{16b}$$

where

$$\begin{aligned} \Gamma_1(\cdot) &= \int_{iT_b}^{iT_b+t_b} \int_{iT_b}^{iT_b+t_b} (\cdot)\, dt_1\, dt_2 \\ \Gamma_2(\cdot) &= \int_{iT_b+\tau_v-\Delta}^{iT_b+t_b} \int_{iT_b+\tau_v-\Delta}^{iT_b+t_b} (\cdot)\, dt_1\, dt_2 \\ \Gamma_3(\cdot) &= \int_{iT_b}^{iT_b+\tau_v-\Delta} \int_{iT_b}^{iT_b+\tau_v-\Delta} (\cdot)\, dt_1\, dt_2 \\ \Gamma_4(\cdot) &= \int_{(i-1)T_b}^{(i-1)T_b+t_b} \int_{iT_b}^{iT_b+t_b} (\cdot)\, dt_1\, dt_2 \\ \Gamma_5(\cdot) &= \int_{(i-1)T_b+\tau_v-\Delta}^{(i-1)T_b+t_b} \int_{iT_b+\tau_v-\Delta}^{iT_b+t_b} (\cdot)\, dt_1\, dt_2 \\ \Re &= R_{l,v}(t_1 - t_2) \\ &= \tfrac{1}{2} E[h_l, v(t_1) h^*_{l,v}(t_2)] \\ \Lambda &= \exp\left[-j2\pi(f_n - f_k) \cdot (t_1 - t_2)\right]. \end{aligned} \tag{16c}$$

As can be seen from (16a), all the first moments depend only on the power of the LOS component whereas the second moments are functions of the correlation coefficients R's. These R's are determined not only by the time selectivity of the channel, that is the fast or slow fading, but also by the frequency selectivity, that is the power delay profile of the channel.

To obtain the SER performance of the kth subchannel, $P_s(k)$ as in (9), the task is to evaluate all the second moments for the different channel conditions. Since Gray bit mapping is assumed

in this paper, the BER of each subchannel can be obtained by dividing $P_s(k)$ in (9) by $\log_2 M$. The BER performance of the whole OFDM-MDPSK system can be obtained by averaging $P_s(k)$ over the entire subchannel assembly as

$$\overline{P}_b = \frac{1}{N \log_2 M} \sum_{k=0}^{N-1} P_s(k). \tag{17}$$

A. Slow Frequency-Selective Rician Fading

For slow fading condition, the channel fluctuation can be neglected during, at least, one multitone block. The $h_{l,v}(t)$ in (4) thus can be modeled as a zero mean complex Gaussian random variable with unity power, and the autocorrelation function in one multitone block is

$$R_{l,v}(t_1 - t_2) = \tfrac{1}{2} E[h_{l,v}(t_1) h^*_{l,v}(t_2)] = 1 \tag{18}$$

where $(i-1)T_b \le t_1, t_2 \le iT_b + t_b$.

Using (18), the coefficient R's in (16a) can be obtained from (7) and (8) as

$$\begin{aligned} R^{(1)}_{S,v} &= R^{(1)}_{C,v} = 1, \quad R^{(2)}_{C,v} = \left(\frac{T_b - \tau_v}{t_b}\right)^2 \\ R^{(2)}_{S,v} &= \left(\frac{T_b - \tau_v}{t_b}\right)^2 + \left(\frac{\tau_v - \Delta}{t_b}\right)^2 \\ &\quad \times \left[-1 + \sum_{n=0}^{N-1} 2 \sin c^2 \left(\frac{(n-k)(\tau_v - \Delta)}{t_b}\right)\right] \end{aligned} \tag{19}$$

where

$$\sin c(x) = \frac{\sin(\pi x)}{\pi x}. \tag{20}$$

The BER of the OFDM-MDPSK system in slow Rician fading channel can now be calculated using (9), (13), (15), (16a), (16b), (16c), (17), and (19).

B. Fast Fading

For fast fading, the $h_{l,v}(t)$ in (4) can be modeled as independent zero-mean complex-valued Gaussian random process whose spectrum $S(f)$ is band-limited to a maximum Doppler shift f_D. Considering a wide sense stationary uncorrelated scattering (WSSUS) channel [4], it is assumed that each diffused multipath component consists of many unresolvable (in delay time) waves which have identical amplitudes and arrive from all direction uniformly. Then, the autocorrelation function of $h_{l,v}(t)$ can be expressed as

$$R_{l,v}(t_1 - t_2) = J_0[2\pi f_D |t_1 - t_2|] \tag{21}$$

where $J_0(\cdot)$ is the zeroth order Bessel function of the first kind, t_1 and t_2 are within two consecutive multitone blocks defined in (18). If $|t_1 - t_2| f_D \ll 1$, (21) can be approximated as [6]

$$R_{l,v}(t_1 - t_2) \approx 1 - \pi^2 f_D^2 (t_1 - t_2)^2. \tag{22}$$

Using (22), the coefficient R's in (16a) can be obtained from (7) and (8) as

$$\begin{aligned} R^{(1)}_{S,v} &= \left(1 - \frac{1}{6}\pi^2 f_D^2 t_b^2\right) + \sum_{\substack{n=0 \\ n \ne k}}^{N-1} \frac{f_D^2 t_b^2}{2(n-k)} \\ R^{(1)}_{C,v} &= 1 - \pi^2 f_D^2 \left(T_b^2 + \tfrac{1}{6} t_b^2\right) \\ R^{(2)}_{S,v} &= U_v(T_b - \tau_v) + U_v(t_b + \tau_v - T_b) \\ &\quad + H_v(T_b - \tau_v) + H_v(t_b + \tau_v - T_b), \\ R^{(2)}_{C,v} &= -\frac{\pi^2 f_D^2}{6 t_b^2} (\tau_v - \Delta)^4 + \frac{2\pi^2 f_D^2}{3 t_b^2} (\tau_v - \Delta)^3 \\ &\quad + \frac{1 - \pi^2 f_D^2 (T_b^2 + t_b^2)}{t_b^2} (\tau_v - \Delta)^2 \\ &\quad + \frac{6\pi^2 f_D^2 t_b T_b^2 + 2\pi^2 f_D^2 t_b^3 - 6 t_b}{3 t_b^2} (\tau_v - \Delta) + R^{(1)}_{C,v} \end{aligned} \tag{23}$$

where

$$\begin{aligned} U_v(x) &= \frac{x^2}{t_b^2} \left(1 - \frac{\pi^2 f_D^2 x^2}{6}\right) \\ H_v(x) &= \sum_{\substack{n=0 \\ n \ne k}}^{N-1} \frac{1}{\pi^2 (n-k)^4} \\ &\quad \left\{ \tfrac{1}{2}(n-k)^2 + \tfrac{3}{4} f_D^2 t_b^2 - 8\pi (n-k) t_b f_D^2 \right. \\ &\quad \cdot x \cdot \sin\left(\frac{2\pi (n-k) x}{t_b}\right) - \frac{1}{4} \\ &\quad \cdot \left[2(n-k)^2 + 3 f_D^2 t_b^2 - 2\pi^2 (n-k)^2 f_D^2 \cdot x^2\right] \\ &\quad \left. \cdot \cos\left(\frac{2\pi (n-k) x}{t_b}\right) \right\}. \end{aligned} \tag{24}$$

The BER of the OFDM-MDPSK system in fast Rician fading can now be calculated using (9), (13), (15), (16a), (16b), (16c), (17), and (23).

IV. BER for Different Power Delay Profiles

From (16a), we note that the BER performance is also determined by the P_v's or the power delay profile. From the first term of I_2 in (8), it can be seen that the delays which are smaller than the guard interval cause ICI only. While from I_3 and the second term of I_2 in (8), the delays which are larger than the guard interval cause both ICI and ISI.

In the following subsections, we consider three different power delay profiles: one-sided exponential, uniform and double spike profiles (see Fig. 2). As defined in (4), the LOS component is separated from the diffused component, and the power delay profiles mentioned above are defined as that of the diffused component only. These power delay profiles are characterized by the average delay $\overline{\tau}$ and the delay spread $\tau_{\rm rms}$, defined as

$$\overline{\tau} = \sum_{v=1}^{V} \frac{P_v}{P_d} \tau_\nu, \quad \tau_{\rm rms} = \sqrt{\sum_{v=1}^{V} \frac{P_v}{P_d} (\tau_v - \overline{\tau})^2}. \tag{25}$$

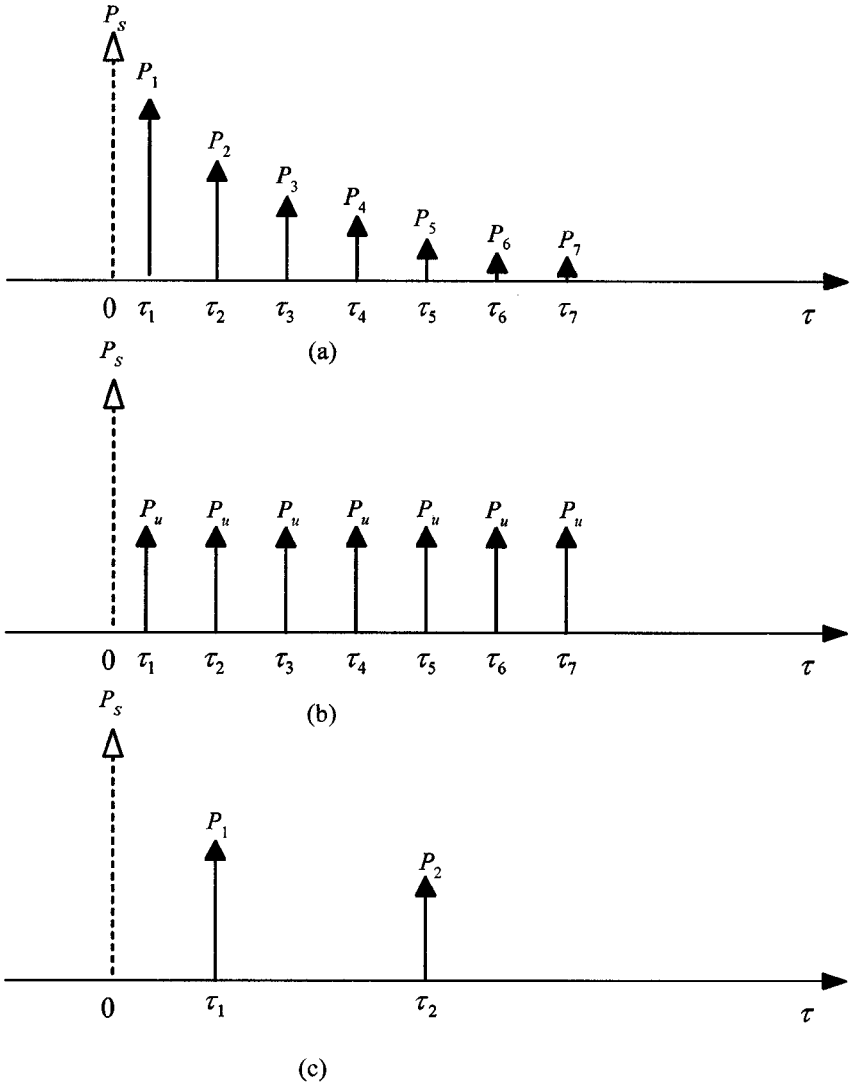

Fig. 2. Power delay profiles: (a) one-sided exponential profile; (b) uniform profile; and (c) double spike profile.

Here, to highlight the effects of channel fading and delay spread, we consider the case of very large signal-to-noise ratio (SNR) in which the AWGN is neglected. The approach used in this paper, however, can be easily extended to take into account of the noise effect. In the case of small SNR, the decision errors will be largely caused by the AWGN, especially for slow fading and small delay spread. As is well known, when the error probability is plotted against the SNR, it levels off to a constant value, called the irreducible error floor, as the SNR becomes very large. The irreducible error probability is the lower bound on the probability of error for all SNR's. However, when the channel is both frequency-selective and time-selective as is the case investigated in this paper, the errors are caused by the ISI which is a result of the frequency selectivity of the channel, and by the ICI which is induced by both the time selectivity and the frequency selectivity of channel. Both interferences result in the loss of orthogonality among the subcarriers. Therefore, in the following analysis, we ignore the AWGN and set $P_n = 0$ in (16a).

A. One-Sided Exponential Profile

The one-sided exponential power delay profile is shown in Fig. 2(a) and can be expressed as

$$g(\tau) = \frac{P_d}{\sum_{m=1}^{V} \exp(-\alpha\tau_m)} \sum_{\nu=1}^{V} \exp(-\alpha\tau)\delta(\tau - \tau_\nu) \qquad (26)$$

where P_d is as defined in (5), and α is an attenuation factor of power delay profile. Therefore,

$$P_\nu = \frac{P_d}{\sum_{m=1}^{V} \exp(-\alpha\tau_m)} \exp(-\alpha\tau_\nu). \qquad (27)$$

After some algebra, the normalized first and second moment expressions for one-sided exponential power delay profile can

be obtained as

$$m_x = \sqrt{K} \cdot c_{k,(i-1)}, \quad m_y = \sqrt{K} \cdot c_{k,i}$$
$$m_{xx} = m_{yy} = \left(\sum_{v=1}^{V_m} Z_v \cdot R_{S,v}^{(1)} + \sum_{v=V_m+1}^{V} Z_v \cdot R_{S,v}^{(2)} \right)$$
$$m_{xy} = \left(\sum_{v=1}^{V_m} Z_v \cdot R_{C,v}^{(1)} + \sum_{v=V_m+1}^{V} Z_v \cdot R_{C,v}^{(2)} \right) \tag{28}$$

where

$$Z_v = \frac{\exp(-\alpha \tau_v)}{\sum_{m=1}^{V} \exp(-\alpha \tau_m)}$$

and the R's can be obtained from (19) and (23) for slow and fast fading, respectively. It should be noted that all the first moments are normalized to $\sqrt{2P_d}$ and the second moments are normalized to $2P_d$.

The first moment m_x, m_y, obviously have the same expressions for these three power delay profiles. Therefore, only the second moments will be obtained in the following sections.

B. Uniform Profile

As shown in Fig. 2(b), the uniform power delay profile is a special case of one-sided exponential profile which has the same power for all diffused multipath components, i.e., $P_v = P_d/V$ when $\alpha = 0$. The delay profile can be expressed as

$$g(\tau) = \frac{P_d}{V} \sum_{\nu=1}^{V} \delta(\tau - \tau_\nu). \tag{29}$$

The second moments needed to calculate the error rate can be obtained as

$$m_{xx} = m_{yy} = \frac{1}{V} \left(\sum_{v=1}^{V_m} R_{S,v}^{(1)} + \sum_{v=V_m+1}^{V} R_{S,v}^{(2)} \right)$$
$$m_{xy} = \frac{1}{V} \left(\sum_{v=1}^{V_m} R_{C,v}^{(1)} + \sum_{v=V_m+1}^{V} R_{C,v}^{(2)} \right). \tag{30}$$

C. Double Spike Profile

The double spike power delay profile is shown in Fig. 2(c) and can be expressed as

$$g(\tau) = \frac{\eta P_d}{1+\eta} \delta(\tau - \tau_1) + \frac{P_d}{1+\eta} \delta(\tau - \tau_2) \tag{31}$$

where η is the ratio of two power spikes, i.e., $\eta = P_1/P_2$.

When τ_2 is larger than the guard interval, the coefficients in (19) and (23) can be simplified by $V_m = 1$ and $V = 2$. Then the normalized second moments for the double spike delay profile can be obtained as

$$m_{xx} = m_{yy} = \left(\frac{\eta}{1+\eta} \right) \cdot R_S^{(1)} + \left(\frac{1}{1+\eta} \right) \cdot R_S^{(2)}$$
$$m_{xy} = \left(\frac{\eta}{1+\eta} \right) \cdot R_C^{(1)} + \left(\frac{1}{1+\eta} \right) \cdot R_C^{(2)}. \tag{32}$$

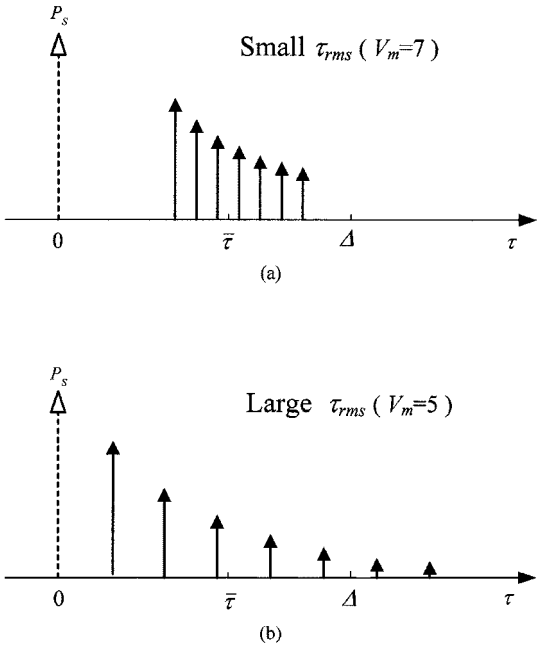

Fig. 3. Illustration highlighting the effect of varying $\tau_{\rm rms}$ on the relative position of the power profiles against the guard interval length Δ, with a constant average delay $\bar{\tau}$.

V. BER Performance as a Function of Delay Spread

In all the numerical results presented in this section, we assume that the average delay $\bar{\tau}$ of the power profile from the LOS component is fixed, while the rms delay spread is varied. Since we have assumed that the interpath delay is uniform, when increasing (decreasing) $\tau_{\rm rms}$, the interpath delay will increase (decrease) accordingly if the number of multipath V is unchanged. In Section III, we have used V_m to indicate the number of paths whose delays are less than the guard interval Δ. As $\tau_{\rm rms}$ is varied, there will be a variation of V_m. When $\tau_{\rm rms}$ is small, it is possible that all the paths have delays which are less than Δ. But as $\tau_{\rm rms}$ is increased, there will be some paths whose delays are larger than Δ. This will lead to an increase in both ICI and ISI and correspondingly an increase of BER. This relation between $\tau_{\rm rms}$, $\bar{\tau}$, V_m and, Δ is highlighted in Fig. 3 for the one-sided exponential delay profile.

In Figs. 4 and 5, the BER performance calculated from (9), (13), and (17) for the one-sided exponential profile is plotted against the normalized rms delay spread $\mu_{\rm rms} = \tau_{\rm rms}/T_b$, and the BER for the three profiles are compared in Fig. 6, with the normalized maximum Doppler shift $f_D T_b$, Rician factor K, and diversity order L as parameters. For all these figures, the number of the subcarriers is 32, the normalized guard interval is $\Delta/T_b = 15\%$ and the average delay is fixed as $\bar{\tau} = 0.8\ \Delta$. For the one-sided exponential profile, we assume that the attenuation factor is $\alpha = 1$, the number of fading paths is $V = 7$ and the interpath delay is uniform. For the uniform profile, $V = 7$ and the interpath delay is uniform also. For the double spike delay profile, the ratio of the two power spikes is $\eta = 2$.

The BER for different OFDM-MDPSK systems with $M = 2, 4, 8$ for the exponential delay profiles are compared in Fig. 4. The curves are for the case of fast fading with $f_D T_b = 0.05$. As

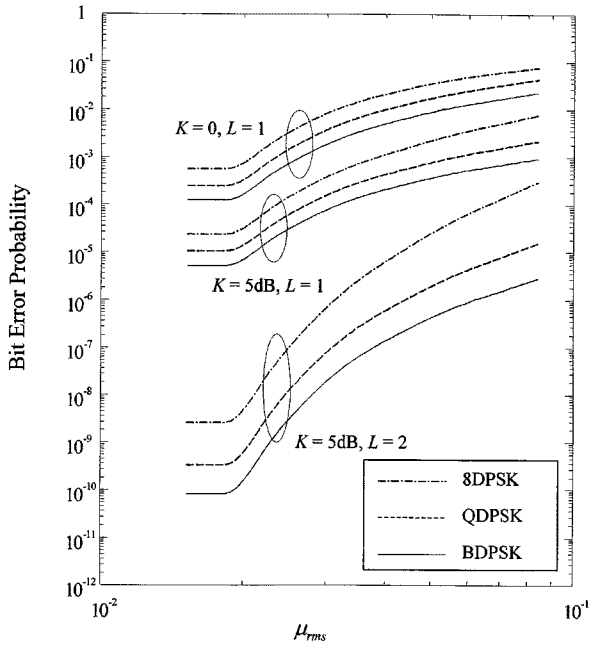

Fig. 4. Average BER of OFDM-MDPSK system in frequency selective Rayleigh and Rician fading with one-sided exponential delay profile with $\alpha = 1, V = 7$, and $f_D T_b = 0.05, N = 32, \Delta/T_b = 0.15, \overline{\tau} = 0.8\Delta$.

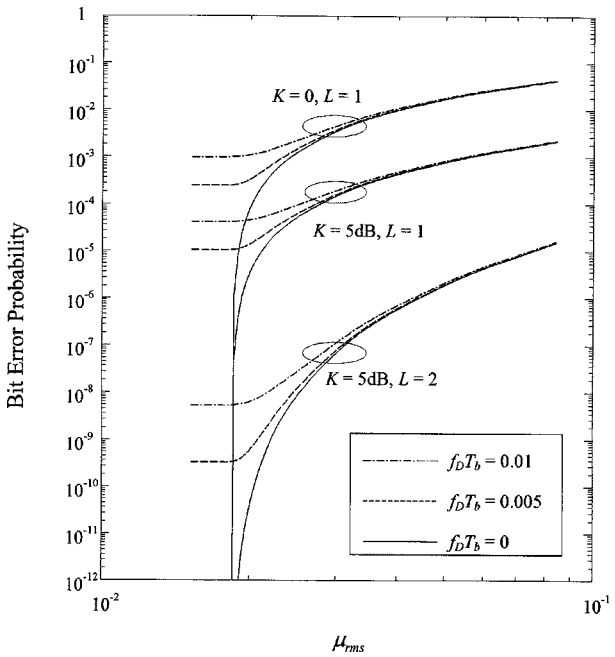

Fig. 5. Average BER of OFDM-QDPSK system in frequency selective Rayleigh and Rician fading with one-sided exponential delay profile with $\alpha = 1, V = 7$, and $M = 4, N = 32, \Delta/T_b = 0.15, \overline{\tau} = 0.8\Delta$.

expected, the BER degraded as $\mu_{\rm rms}$ is increased. In the comparison of performance between the different M, since we have assumed that T_b is fixed, the system with a larger M is associated with a larger input binary data rate which implies that the system has a larger spectral efficiency in term of bit/s/Hz.

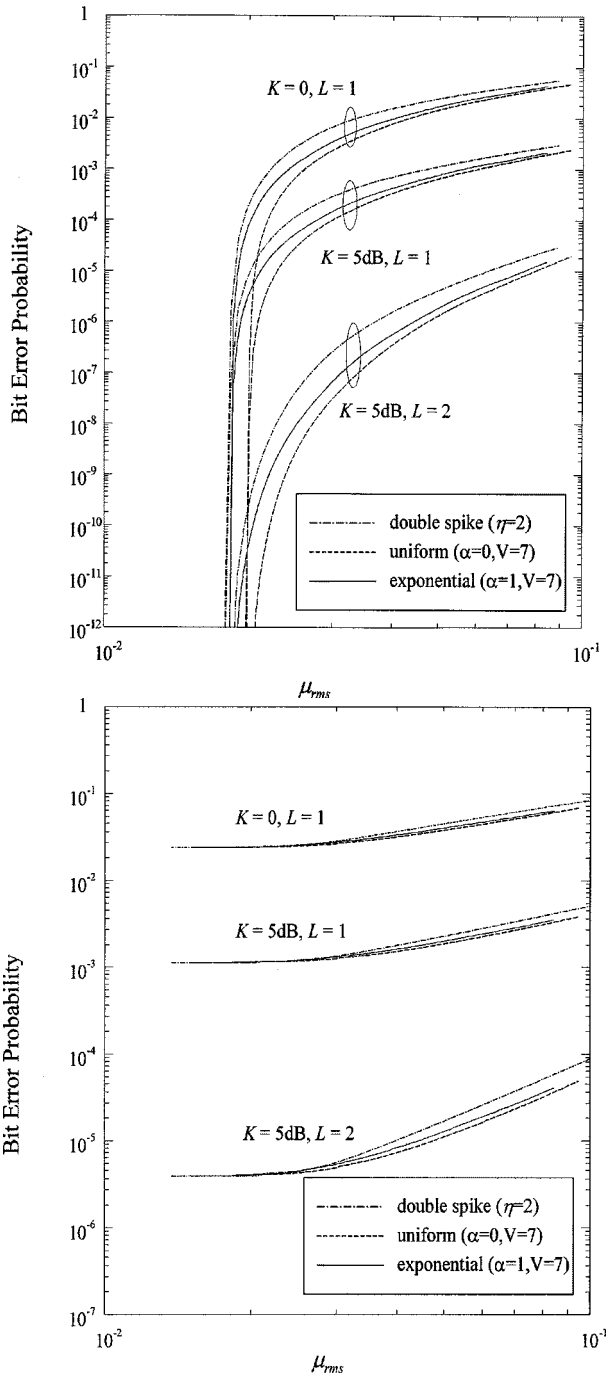

Fig. 6. (a) Average BER of OFDM-QDPSK system in frequency selective Rayleigh and Rician fading with $M = 4, f_D T_b = 0, N = 32, \Delta/T_b = 0.15, \overline{\tau} = 0.8\Delta$. (b) Average BER of OFDM-QDPSK system in frequency selective Rayleigh and Rician fading with $M = 4, f_D T_b = 0.05, N = 32, \Delta/T_b = 0.15, \overline{\tau} = 0.8\Delta$.

As expected the system with a larger M has a poorer BER performance. Also, the Rician fading leads to a better BER performance than the Rayleigh fading, because of the existence of the unfaded specular component. By comparing the curves with $L = 1$ and $L = 2$, we can see that the use of diversity reception is effective in improving the BER performance.

We show in Fig. 5 the BER for $M = 4$, to highlight the unique behavior for the slow fading case $(f_D T_b = 0)$. As $\mu_{\rm rms}$ is reduced, the BER decreases gradually and then when reaching

$\mu_{\rm rms} \cong 0.02$, it drops off steeply to zero. This can be explained as follows. For the specified parameter values of $V = 7$, $\Delta/T_b = 0.15$, and $\overline{\tau} = 0.8\Delta$, it can be shown from (25) and (26) that all the path delays are less than Δ for $\mu_{\rm rms} \cong 0.02$. Therefore, as stated in the beginning paragraph of Section IV, there will be no ISI. Furthermore, since $f_D T_b = 0$, there will be no ICI in this case (see Appendix A.) Finally since AWGN have been neglected, the BER should approach zero. However, when $f_D T_b \neq 0$, for $\mu_{\rm rms} \leq 0.02$, although ISI is zero, there will still be ICI which lead to some finite BER, as can be seen in Fig. 5, for $f_D T_b = 0.005$ and $f_D T_b = 0.01$. The BER curves for $\mu_{\rm rms} \leq 0.02$ stay constant as $\mu_{\rm rms}$ varies. This is because the contribution from the ICI to the BER is not a function of τ_ν (seeAppendix B.)

In Fig. 6, the BER performance with three different power delay profiles is presented. Fig. 6(a) is for slow fading, and Fig. 6(b) is for fast fading. In the fast fading case, the BER performance are similar given that the $\overline{\tau}$ and $\tau_{\rm rms}$ are the same for all the three profiles. The same is true in the slow fading condition when $\tau_{\rm rms}$ is large.

VI. Conclusions

This paper is concerned with the BER performance of OFDM-MDPSK system in frequency-selective Rayleigh and Rician fading channels with diversity reception. One of the new contributions is our recognition that the classic formula of Proakis [3, Appendix B] relating to the probability, that the sum of L pairs of complex valued Gaussian random variables is less than zero, can be used to obtain a closed form expression of the BER performance of OFDM-MDPSK systems. New BER results computed from our derived formula are used to quantitatively illustrate the effect of frequency selectivity and time selectivity of the mobile radio channels on the system performance. The existence of a strong LOS component and the use of diversity reception are effective in improving transmission performance.

Appendix A

In the slow fading channel ($f_D T_b = 0$), when all the path delays are less than the guard interval, Δ, ($V_m = V$), there is no ICI. This can be seen as follows. Firstly, by referring to (18): when $f_D T_b = 0$, $R_{l,v}(t_1 - t_2) = 1$, which implies that $h_{l,v}(t)$ is a constant. Next, by looking back at (8), the ICI is represented by

$$I_2 = \sum_{\substack{n=0 \\ n\neq k}}^{N-1} \frac{c_{n,i}}{t_b} \cdot \left\{ \sum_{v=1}^{V_m} e^{-j2\pi f_n \tau_v} \sqrt{P_v} \int_{iT_b}^{iT_b+t_b} h_{l,v}(t) \times e^{-j2\pi(f_n - f_k)(t-iT_b)}\, dt + \sum_{v=V_m+1}^{V} e^{-j2\pi f_n \tau_v} \times \sqrt{P_v} \int_{iT_b+\tau_v-\Delta}^{iT_b+t_b} h_{l,v}(t) e^{-j2\pi(f_n - f_k)(t-iT_b)}\, dt \right\}.$$

This consists of two terms. The second term is zero, because all the path delays are less than guard interval Δ. The first term is zero, because $h_{l,v}(t)$ is a constant and the subcarriers with frequencies f_n and f_k are orthogonal over a multitone block of length t_b.

Appendix B

In the fast fading channel ($f_D T_b \neq 0$), when all the path delays are less than the guard interval, Δ, ($V_m = V$), then BER does not vary as $\mu_{\rm rms}$ is changed. This can be seen as follows. In (16a), the m_{xx}, m_{yy} and m_{xy} only depend on $R^{(1)}_{C,V}$ and $R^{(1)}_{S,V}$. From (23), $R^{(1)}_{C,V}$ and $R^{(1)}_{S,V}$ do not depend on τ_ν, that is on the power profile and accordingly $\mu_{\rm rms}$. Therefore the BER is constant when $\mu_{\rm rms}$ is changed.

References

[1] M. Okada, S. Hara, and N. Morinaga, "Bit error rate performance of orthogonal multicarrier modulation radio transmission systems," *IEICE Trans. Commun.*, vol. E76-B, no. 2, pp. 113–119, Feb. 1993.

[2] M. Saito, S. Moriyama, S. Nakahara, and K. Tsuchida, "Transmission characteristics of DQPSK-OFDM for terrestrial digital broadcasting systems," *IEICE Trans. Commun.*, vol. E77-B, no. 12, pp. 1451–1459, Dec. 1994.

[3] J. G. Proakis, *Digital Communications*, 3rd ed. New York: McGraw-Hill, 1995.

[4] R. Steele, *Mobile Radio Communications*. London, U.K.: Pentech Press, 1992.

[5] T. S. Rappaport, *Wireless Communications: Principles and Practice*. Englewood Cliffs, NJ: Prentice-Hall, 1996.

[6] W. C. Lee, *Mobile Communications Engineering*. New York: McGraw-Hill, 1982.

[7] A. Vahlin and N. Holte, "OFDM for broadcasting in presence of analogue co-channel interference," *IEEE Trans. Broadcast.*, vol. 41, pp. 89–93, Sept. 1995.

[8] M. Alard and R. Lassalle, "Principles of modulation and channel coding digital broadcasting for mobile receivers," *EBU Review—Technical*, no. 224, p. 47, Aug. 1989.

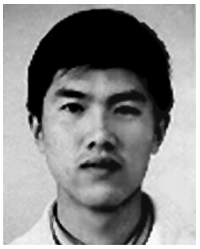

Jun Lu received the B.Eng. degree from the Xi'an Jiao Tong University, Xi'an, China, in 1992, the M.Eng. degree from the Shanghai Jiao Tong University, Shanghai, China, in 1995, and the Ph.D. degree from the National University of Singapore, Singapore, in 1998. All his degrees are in electrical engineering.

Since 1997, he has been a Senior Research Engineer, Staff Research Engineer, and then Member of Technical Staff at the Center of Wireless Communications, Singapore. His research interests include digital wireless communications, digital signal processing, and ASIC design.

Tjeng Thiang Tjhung (SM'84) received the B.Eng. and M.Eng. degrees in electrical engineering from Carleton University, Ottawa, Ont., Canada, in 1963 and 1965, respectively, and the Ph.D. degree from Queen's University, Kingston, Ont., in 1969.

From 1963 to 1968, he was at Acres-Inter-Tel Ltd., Ottawa, as a Consultant, where his work was concerned with FSK systems for secure radio communication. In 1969, he joined the Department of Electrical Engineering, National University of Singapore, Singapore, where he is currently a Professor. His present research interests are in bandwidth-efficient digital modulation techniques for mobile radio and in multicarrier and code-division multiple-access communication systems. From 1977 to 1983, he was a Consultant to Singapore Telecom on the planning and implementation of their optical fiber wide-band network.

Dr. Tjhung is a Member of the IEICE Japan and a Fellow of IES Singapore. He is also a Member of the Association of Professional Engineers of Singapore.

Fumiyuki Adachi (M'79–SM'90) received the B.S. and Dr.Eng. degrees in electrical engineering from Tohoku University, Sendai, Japan, in 1973 and 1984, respectively.

In 1973, he joined the Electrical Communications Laboratories of Nippon Telegraph and Telephone Corporation (now, NTT) and conducted various research related to digital cellular mobile communications. Since 1992, he has been with NTT Mobile Communications Network, Inc., Yokosuka-shi, Japan, where he is a Senior Executive Research Engineer and Director of the Wireless Access Laboratory. Currently, he is leading a research group on wideband wireless access for IMT2000 and beyond. His research interests include: wideband/broadband CDMA, spreading code design, Rake and space diversity reception techniques, adaptive antenna array, and bandwidth efficient modulation and channel coding techniques. During the academic year of 1984–1985, he was a United Kingdom SERC Visiting Research Fellow in the Department of Electrical Engineering and Electronics at Liverpool University. Since 1997, he has been a Visiting Professor at Nara Institute of Science and Technology, Japan. He has written chapters of three books: *Fundamentals of Mobile Communications* (published in Japanese by IEICE, 1986), *Mobile Communications* (published in Japanese by Maruzen Publishing Co., Tokyo, Japan, 1989), and *Digital Mobile Communications* (published in Japanese by Kagaku Shinbun-sha, Tokyo, Japan, 1992).

Dr. Adachi was a co-recipient of the IEEE Vehicular Technology Transactions Best Paper of the Year Award 1980 and again 1990. He is a member of IEICE of Japan and was a co-recipient of the IEICE Transactions Best Paper of the Year Award in 1996 and 1998.

Li Cheng Huang received the B.Eng. degree in electronics engineering from Nanjing University of Aeronautics and Astronautics, Nanjing, China, in 1994. He studied image processing in Beijing University of Aeronautics and Astronautics, Beijing, China, from 1996 to 1998, and he is currently pursuing the Ph.D. degree in electrical engineering at National University of Singapore, Singapore.

From 1994 to 1996, he was an Engineer at the Chinese Aeronautics Radio Research Institute, where his work was concerned with Global Positioning System. His current research interests are digital mobile communications systems, multicarrier communications systems, error-correcting coding performance, and channel estimation.